A New Design Concept for Low-Loss SAW Filters Based on Different-Width Split-Finger SPUDT

Hiroyuki Nakamura, *Member, IEEE*, Toru Yamada, *Member, IEEE*, Toshio Ishizaki, *Senior Member, IEEE*, and Kazunori Nishimura

***Abstract*—A new design concept of a single-phase unidirectional transducer (SPUDT) has been investigated in this paper. The concept has been realized by using a newly developed different-width split-finger–SPUDT structure, in which the adjacent electrode fingers are given different widths. A symmetrical radiation conductance is obtained by adjusting the electrode finger positions. Computer simulations have confirmed that the electrical $1/Q$ factor and the directivity have a tradeoff relationship with regard to the finger-width ratio, depending on the metallization thickness used. From the simulation results, the optimum finger-width ratio for achieving a low insertion loss has been obtained. An experimental filter was constructed, which shows good performance, with the insertion loss improved by 1 dB when compared to a conventional electrode-width-controlled–SPUDT filter on an ST-cut quartz substrate.**

***Index Terms*—Low-loss filters, SAW mobile radio filters, SPUDT.**

I. Introduction

RECENTLY, the single-phase unidirectional transducer (SPUDT) technique has been developed and is now widely used in surface acoustic wave (SAW) filter designs for various code-division multiple-access (CDMA) applications. Filters for such applications need to have good performance characteristics, such as a low insertion loss, a wide passband, a high rejection near passband, flat passband characteristics, and need to exhibit a miniaturized size.

The performance of filters using a bidirectional transducer is degraded by the triple-transit echo, and the insertion loss is also increased by bidirectional propagation loss. The SPUDT technique can suppress the triple-transit echo, using reflections within the transducers, and can improve the insertion loss owing to its inherent unidirectional directivity [1]–[3]. In the design of the SPUDT, the localized centers of excitation are displaced by $\lambda/8$ from the localized centers of reflection. Various SPUDT structures such as the distributed acoustic reflection transducer (DART) SPUDT [4], electrode-width controlled (EWC)–SPUDT [5], Hunsinger-geometry SPUDT [6], dithered SPUDT (DSPUDT) [7] have been already reported. Fig. 1 shows the structure of the EWC–SPUDT. It consists of three electrode fingers per wavelength, with one $\lambda/4$ width electrode and two $\lambda/8$ width electrodes in a unit length. It is well known that this structure has a unidirectional performance and symmetrical radiation conductance since there is a $\lambda/8$ phase difference between the center of the excitation and center of reflection [5], [8]. An analysis of the electrical $1/Q$ factor for application to the passband characteristics of the SPUDT has been reported [9], [10]. The effective electromechanical coupling constant has been observed to be related to the electrical $1/Q$ factor [11]. However, there has been no evaluation reported for the insertion loss of the SPUDT from the point-of-view where both the electrical $1/Q$ factor and directivity are considered as a function of the finger-width ratio. This ratio is defined as the width of the wide finger divided by that of the narrow finger.

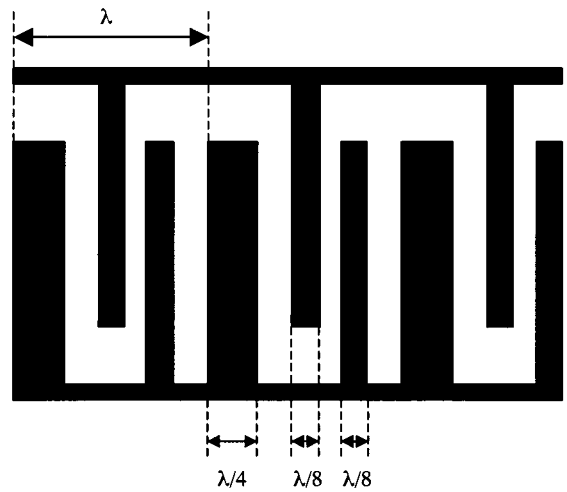

Fig. 1. Configuration of the EWC–SPUDT.

In this paper, a new design concept for improving the tradeoff relation between the electrical $1/Q$ factor and the directivity of a different-width split-finger (DWSF)–SPUDT on an ST-cut quartz substrate is studied. The DWSF–SPUDT has four electrodes per wavelength. The adjacent electrode fingers have different widths. The filter performance can be controlled by the finger-width ratio. The electrode finger positions may be adjusted to obtain a symmetrical radiation conductance. The filters have then been characterized as a function of the finger-width ratio and the metallization thickness. For the DWSF–SPUDT, the insertion loss is analyzed incorporating both the electrical $1/Q$ factor and the directivity. The optimum finger-width ratio for minimizing the insertion loss depends on the normalized metallization thickness. As a result, the insertion loss of the DWSF–SPUDT has been improved by 1 dB in comparison with a conventional EWC–SPUDT filter.

Manuscript received October 13, 2000; revised January 14, 2001.

H. Nakamura, T. Yamada, and T. Ishizaki are with the Matsushita Electric Industrial Corporation Ltd., Osaka 571-8501, Japan.

K. Nishimura is with the Matsushita Electronic Components Corporation Ltd., Osaka 571-8506, Japan.

Publisher Item Identifier S 0018-9480(01)02901-5.

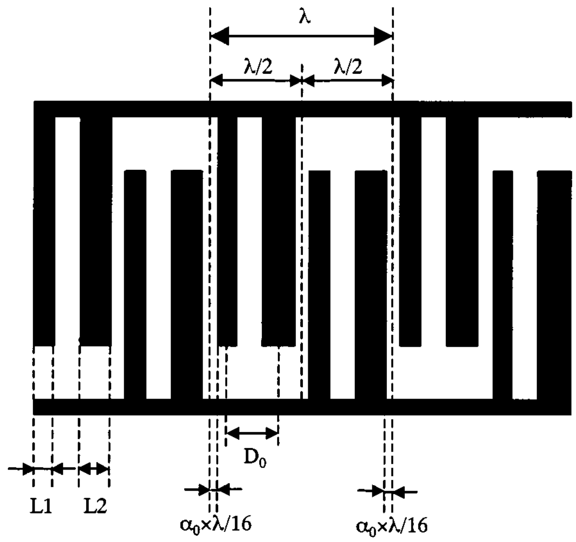

Fig. 2. Configuration of the DWSF–SPUDT.

The structure of the proposed the DWSF–SPUDT will be presented first. The adjustment method of electrode finger positions will then be explained. Subsequently, we compare the electrical $1/Q$ factor and the directivity of the DWSF SPUDT with that of a conventional EWC–SPUDT. We then present optimization results for the finger-width ratio carried out by computer simulations. Finally, the insertion loss of an experimental filter will be reported.

II. Configuration of the DWSF–SPUDT Filter

A. Configuration of the DWSF–SPUDT

Fig. 2 shows the structure of the DWSF–SPUDT [12]. The DWSF–SPUDT has four electrode fingers per wavelength. The adjacent electrode fingers have different widths, respectively. The wide finger ($L2$) and the narrow finger ($L1$) are placed alternatively. The directivity is obtained by adjusting the phase difference between the center of excitation and the center of reflection. The filter performance is controlled by the finger-width ratio ($L2/L1$), defined as the width of the wide finger divided by that of the narrow finger. In this figure, the DWSF–SPUDT with $L2/L1 = 1.0$ contains $\lambda/8$-width bidirectional transducers, which is generally called a "split-finger" arrangement. In the DWSF–SPUDT, the electrical $1/Q$ factor is controlled by the finger-width ratio. Furthermore, the finger-width ratio changes the reflection in the electrodes and, therefore, the directivity of the SPUDT can be adjusted by varying this parameter.

The $\lambda/8$ phase difference between the center of excitation and the center of reflection of the SPUDT is very important for obtaining symmetrical characteristics for the filter responses [8]. In the DWSF–SPUDT, the phase difference is changed by the finger-width ratio, thus, an adjustment of the electrode finger positions is required to obtain symmetrical filter characteristics. When designing the DWSF–SPUDT, the finger position parameter α_0 can be varied to give a symmetrical radiation conductance, as shown in Fig. 3. This figure shows the radiation conductance (G) with $\alpha_0 = 0.44$, as compared with $\alpha_0 = 1.00$, for a design with a normalized metallization thickness (h/λ) of 1.4%, and with the number of electrode finger pairs equal to 100. The sum of both finger widths ($L1 + L2$) was $\lambda/4$, and the finger-width ratio ($L2/L1$) was 3.0. Here, the DWSF–SPUDT of $\alpha_0 = 1.00$ means Hunsinger-geometry SPUDT. The vertical axis is normalized to the maximum value of the radiation conductance. In the Hunsinger-geometry SPUDT, $\alpha_0 = 1.00$, the center-to-center spacing is $\lambda/4$, and a radiation conductance was asymmetrical. In the DWSF–SPUDT, a symmetrical radiation conductance can be obtained by using $\alpha_0 = 0.44$. Fig. 4 shows the α_0 characteristics as a function of the finger-width ratio. The choice of α_0 value has introduced two peaks on both sides of the center frequency in the radiation conductance with the same level. The α_0 value decreases with the finger-width ratio. The center-to-center spacing (D_0) between the wide and narrow finger is changed with respect to the finger-width ratio, as shown in (1). If $L1 + L2 = \lambda/4$ and $L2/L1 = 3.0$, the D_0 spacing is about 0.32λ, using $\alpha_0 = 0.44$ in Fig. 4. Therefore, the phase difference of the DWSF–SPUDT can be adjusted by using just only one parameter, i.e., the α_0 value, as follows:

$$D_0 = \frac{\lambda}{2} - \frac{L1 + L2}{2} - \frac{\alpha_0 \times \lambda}{8}. \quad (1)$$

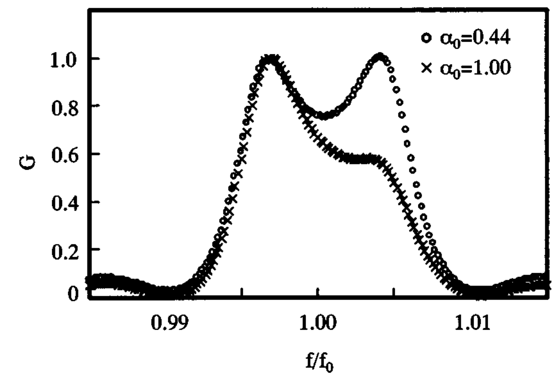

Fig. 3. Normalized radiation conductance of the DWSF–SPUDT with $\alpha_0 = 0.44$ and $\alpha_0 = 1.00$.

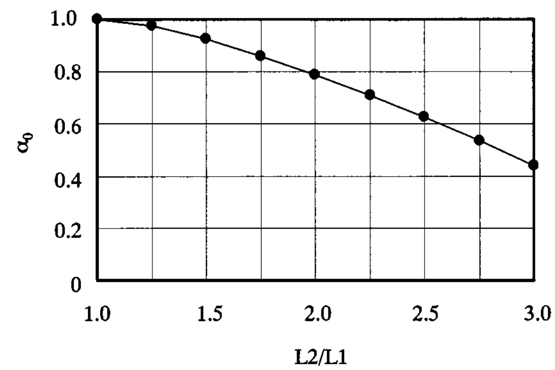

Fig. 4. α_0 characteristics as a function of the finger-width ratio.

B. Combination of the DWSF–SPUDT and $\lambda/8$ Split Fingers

$\lambda/8$ split fingers are incorporated into the DWSF–SPUDT in order to achieve a practical filter design. The center of excitation of the DWSF–SPUDT has to be consistent with that of the $\lambda/8$ split fingers in every $\lambda/2$ periodic space. In this case, two finger position parameters, i.e., α and β, as defined in Fig. 5,

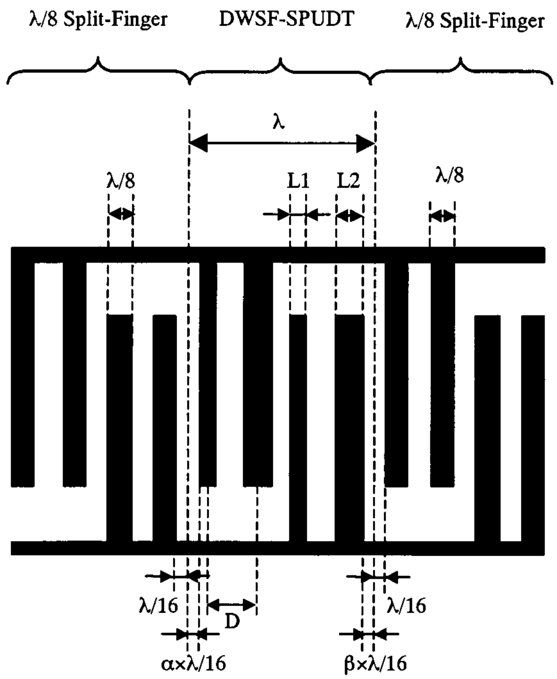

Fig. 5. Combination of the DWSF–SPUDT with the $\lambda/8$ split fingers.

have to be introduced. Fig. 5 shows the structure of the combination of the DWSF–SPUDT and the $\lambda/8$ split fingers. The α- and the β-parameters in Fig. 5 are the position parameters of the narrow and wide fingers, respectively. The α and β values we have chosen have introduced two peaks on both sides of the center frequency in the radiation conductance with the same level. Fig. 6 shows the radiation conductance of the combination of the DWSF–SPUDT and the $\lambda/8$ split fingers. The number of the DWSF–SPUDT pairs is 100 and the number of the $\lambda/8$ split-finger pairs is 50. Fig. 6(a) shows the radiation conductance without the adjustment of the electrode finger positions. Here, the normalized metallization thickness (h/λ) is 1.4%, and $L2/L1 = 3.0$, $L1 + L2 = \lambda/4$. The α and β values are the same in the case of the DWSF–SPUDT alone. This means that $\alpha = \beta = \alpha_0 = 0.44$. The radiation conductance is asymmetrical because of nonperiodicity between the centers of the excitation between the DWSF–SPUDT and the $\lambda/8$ split fingers. Fig. 6(b) shows the variation of the radiation conductance with adjustment of the electrode finger positions $\alpha = 0.17$ and $\beta = 0.71$. As shown in Fig. 6(b), a symmetrical radiation conductance can be obtained by adjusting the two electrode position parameters. The centers of excitation of the DWSF–SPUDT and those of the $\lambda/8$ split fingers then become periodically placed.

The centers of excitation and centers of reflection are shifted according to the normalized metallization thickness and the finger-width ratio. Fig. 7 shows the α and β characteristics as a function of the finger-width ratio for different normalized metallization thickness. In Fig. 7, the normalized metallization thicknesses are 1.0%, 1.4%, and 1.8%. The α and β values clearly depend on the normalized metallization thickness and the finger-width ratio. It is considered that a change in the electrode reflection caused by a change in the normalized metallization thickness or by the finger-width ratio has an influence on the phase difference. Thus, the center-to-center

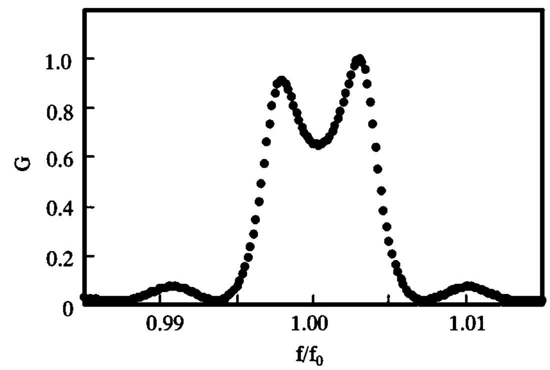

(a)

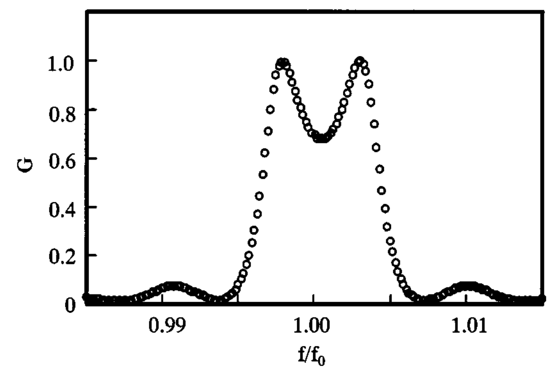

(b)

Fig. 6. Normalized radiation conductance for the combination of the DWSF–SPUDT with the $\lambda/8$ split fingers. (a) Shows the conductance in the case of $\alpha = \beta = \alpha_0 = 0.44$ and (b) in the case of $\alpha = 0.17$ and $\beta = 0.71$.

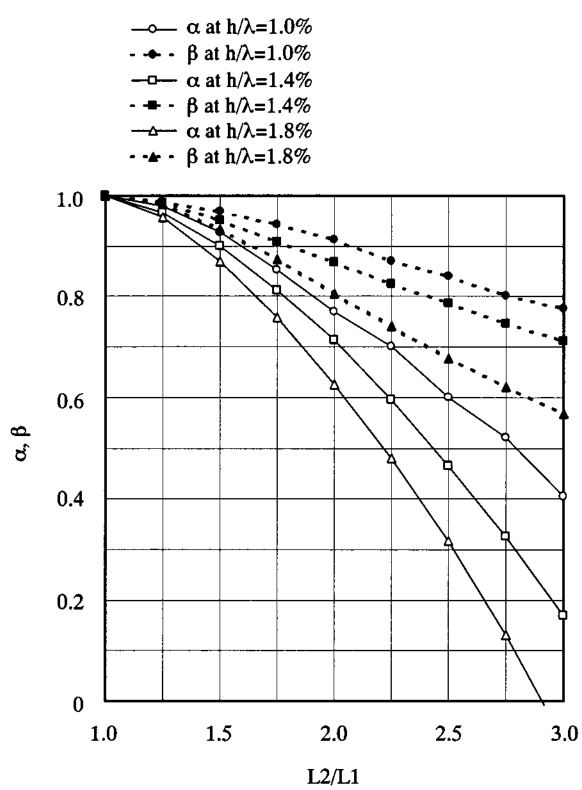

Fig. 7. Characteristics of the α and β parameters as a function of the finger-width ratio ($L2/L1$) at $h/\lambda = 1.0\%$, 1.4%, and 1.8%.

spacing (D) between the wide and narrow fingers is changed by the finger-width ratio as (3). Here, the electrode position finger parameters satisfy (3). The α value has to be less than the β value in order to obtain a symmetrical radiation conductance

$$D = \frac{\lambda}{2} - \frac{L1 + L2}{2} - \frac{(\alpha + \beta) \times \lambda}{16} \quad (2)$$

$$2 \times \alpha_0 = \alpha + \beta, \qquad \alpha < \beta. \quad (3)$$

It is very important for the performance of the DWSF–SPUDT to determine the optimum electrode finger positions. In the DWSF–SPUDT, both the narrow and wide fingers reflect the acoustic wave. The correct placement of the electrode finger positions improves the symmetry of the radiation conductance and then excellent filter characteristics can be obtained.

III. Computer Analysis of the DWSF–SPUDT Filter

A. *Electrical* $1/Q$ *Factor of DWSF–SPUDT*

The electrical $1/Q$ factor of the transducer is expressed as the ratio of the radiation conductance (G) and the capacitance (C) [9], [10]. Here, ω is $2\pi f$, where f is the frequency

$$1/Q = \frac{G}{\omega C}. \quad (4)$$

The electrical $1/Q$ factor, defined by the Smith equivalent model [10], is proportional to the effective electromechanical coupling constant of the transducers. Thus, as the electrical $1/Q$ factor increases, the effective electromechanical coupling constant becomes large. The efficiency of generating SAWs then becomes large. Therefore, increasing the electrical $1/Q$ factor has the effect of lowering the insertion loss of the SAW filter. For the computer analysis of the filter characteristics, a P-matrix model was used. The electrical $1/Q$ factor and directivity of the DWSF–SPUDT were analyzed as a function of the finger-width ratio. The results are compared with those of a conventional EWC–SPUDT. Fig. 8 shows the electrical $1/Q$ factor versus the finger-width ratio. The electrical $1/Q$ factor is normalized to that of the $\lambda/8$ split fingers with $L2/L1 = 1.0$. The normalized metallization thickness is 1.5%, and the number of transducer electrode pairs is 100. A metallization ratio is 0.5, which means $L1 + L2 = \lambda/4$ for the DWSF–SPUDT. In Fig. 8, the dashed line shows the electrical $1/Q$ factor of the conventional EWC–SPUDT under the same conditions. The electrical $1/Q$ factor of the DWSF–SPUDT decreases with increasing the finger-width ratio. In this situation, reflection by the wide fingers is increased, resulting in a reduced radiation conductance. The capacitance also becomes larger as the finger ratio increases, due to the capacitance increase of the transducers. Fig. 9(a) and (b) shows the radiation conductance and capacitance as a function of the finger-width ratio, respectively. Here, the radiation conductance and capacitance are normalized to those of a bidirectional transducer with $L2/L1 = 1.0$. The dashed lines of this figure represent the characteristics of the EWC–SPUDT. Fig. 8 illustrates the relationship between the electrical $1/Q$ factor and the finger-width ratio for both types of SPUDTs. It is clear that the electrical $1/Q$ factor of the DWSF–SPUDT is significantly improved with respect to the EWC–SPUDT in the region of $L2/L1 < 2.7$.

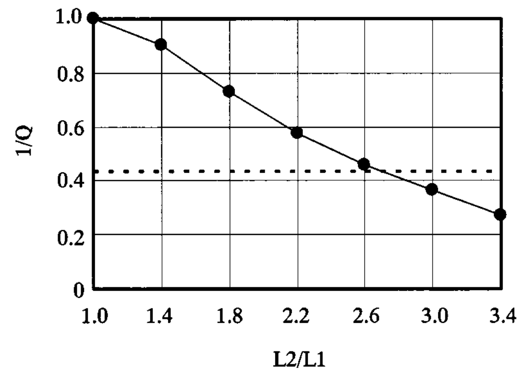

Fig. 8. Characteristics of the normalized electrical $1/Q$ factor as a function of the finger-width ratio ($L2/L1$) at $h/\lambda = 1.5\%$. The dashed line indicates the characteristics of the EWC–SPUDT for comparison.

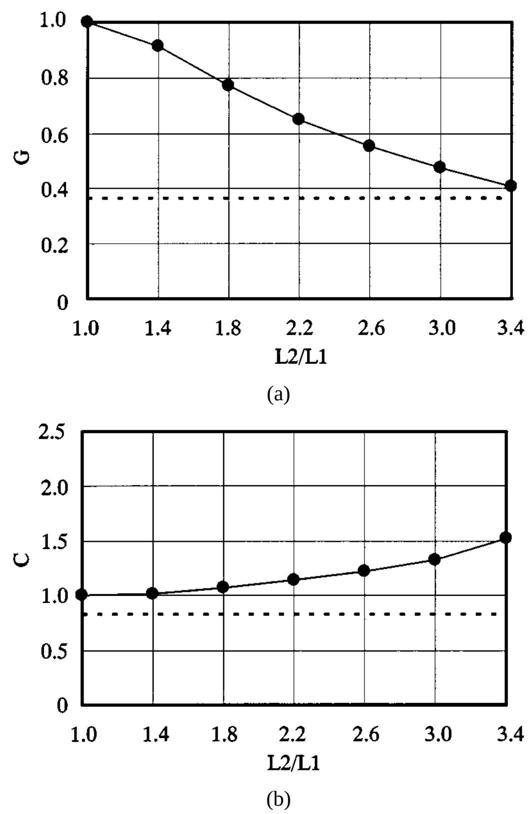

Fig. 9. Characteristics of: (a) the normalized conductance and (b) normalized capacitance as a function of the finger-width ratio ($L2/L1$) at $h/\lambda = 1.5\%$. The dashed line indicates the characteristics of the EWC–SPUDT for comparison.

B. *Directivity of the DWSF–SPUDT*

Fig. 10 shows the directivity characteristics of the DWSF–SPUDT as a function of the finger-width ratio. The normalized metallization thickness is 1.5% and the number of transducer electrode pairs is 100. The dashed line shows the directivity of the EWC–SPUDT under the same conditions. The directivity increases with the finger-width ratio, due to increasing reflection by the wide fingers. The EWC–SPUDT has one $\lambda/4$ width electrode per wavelength, which contributes

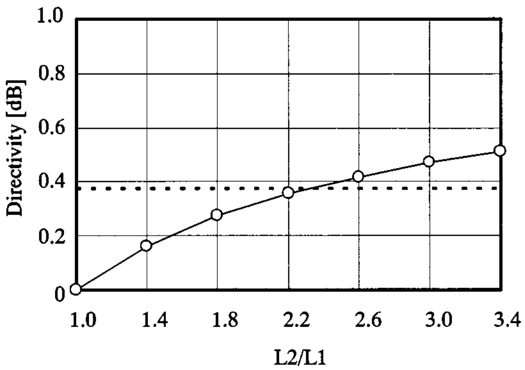

Fig. 10. Characteristics of the directivity as a function of the finger-width ratio ($L2/L1$) at $h\lambda = 1.5\%$. The dashed line indicates the characteristics of the EWC–SPUDT for comparison.

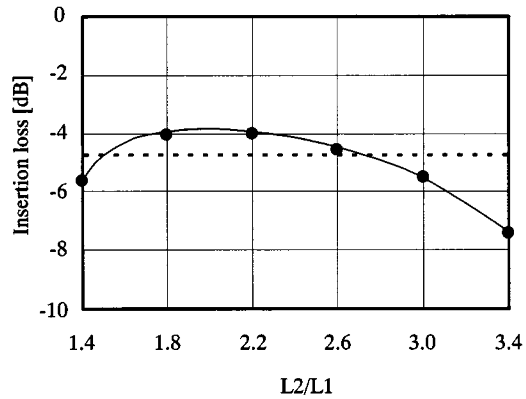

Fig. 11. Characteristics of the insertion loss as a function of the finger-width ratio ($L2/L1$) at $h/\lambda = 1.5\%$. The dashed line indicates the characteristics of the EWC–SPUDT for comparison.

to the reflections, while the DWSF–SPUDT has two wide fingers in a wavelength, where the width of the wide finger is $\lambda/8 < L2 < \lambda/4$. Therefore, the total reflection of the DWSF–SPUDT is larger than that of the EWC–SPUDT. Therefore, the DWSF–SPUDT with $L2/L1 > 2.4$ gives larger directivity than the equivalent EWC–SPUDT.

C. Insertion Loss of the DWSF–SPUDT

The electrical $1/Q$ factor decreases with the finger-width ratio and the directivity increases with the finger-width ratio. Therefore, regarding the insertion loss, the above two factors have a tradeoff relation. An optimum finger-width ratio should exist to minimize the insertion loss. Fig. 11 shows the simulated insertion loss as a function of the finger-width ratio. Two SPUDT filters are placed side-by-side with opposing directivities. The normalized metallization thickness was 1.5% and the number of transducer pairs was 100. In Fig. 11, the dashed line indicates the insertion loss of the EWC–SPUDT under the same conditions. In the region of the small finger-width ratio, although the electrical $1/Q$ factor is large, the directivity is small. The DWSF–SPUDT does not give improved insertion loss in this region. In the region of large finger-width ratio, although the directivity is large, the electrical $1/Q$ factor is small. The DWSF–SPUDT also does not improve the insertion loss in this region. However, in the region with a finger-width ratio of $1.5 < L2/L1 < 2.7$, the DWSF–SPUDT can improve the insertion loss due to a satisfactory tradeoff between the electrical $1/Q$ factor and directivity. In particular, the use of finger-width ratios of $1.8 < L2/L1 < 2.2$ can give excellent insertion losses. Our observation of region of loss minimization allows the design of optimum low-loss filters.

D. Parameter Dependence on the Metallization Thickness

The electrical $1/Q$ factor and directivity both depend on the metallization thickness. The optimum finger-width ratio, which minimizes the insertion loss, might be different depending on the metallization thickness. First, the electrical $1/Q$ factor and the directivity as a function of the metallization thickness have been simulated. Fig. 12 shows the finger-width ratio as a function of metallization thickness under conditions where the DWSF–SPUDT and EWC–SPUDT both have the same electrical $1/Q$ factor. In the region of the finger-width ratio below the solid line, the DWSF–SPUDT has the larger electrical $1/Q$ factor compared with that of EWC–SPUDT. The finger-width ratio, which improves the electrical $1/Q$ factor, decreases with the metallization thickness.

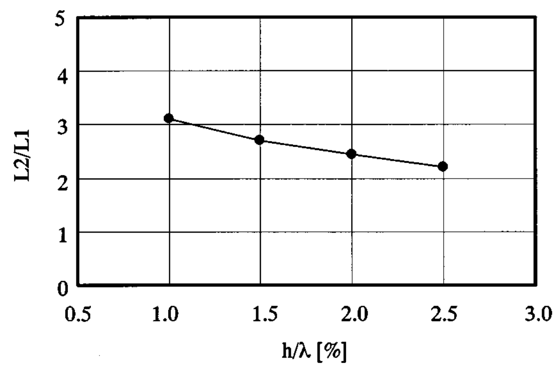

Fig. 12. Finger-width ratio for both types of SPUDTs, where the EWC and DWSF SPUDTs have the same electrical $1/Q$ factor, as a function of h/λ.

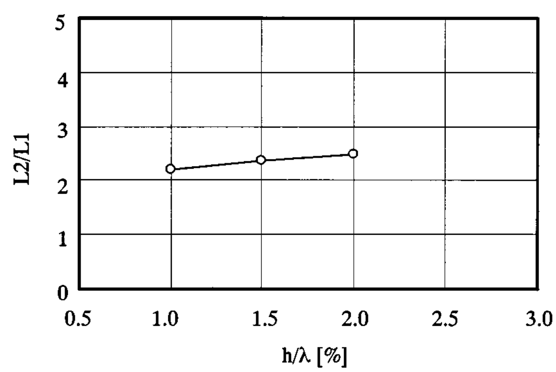

Fig. 13. Finger-width ratio for both types of SPUDTs, where the EWC and DWSF SPUDTs have the same directivity, as a function of the h/λ.

Fig. 13 shows the finger-width ratio dependence on the metallization thickness, under conditions where the DWSF–SPUDT and EWC–SPUDT have the same directivity. In the region of the finger-width ratio below the solid line, the DWSF–SPUDT has a smaller directivity compared with that of the EWC–SPUDT. The directivity of the DWSF–SPUDT is smaller than that of the EWC–SPUDT, when the parameters are $h/\lambda = 2.5\%$ and $L2/L1 < 2.2$.

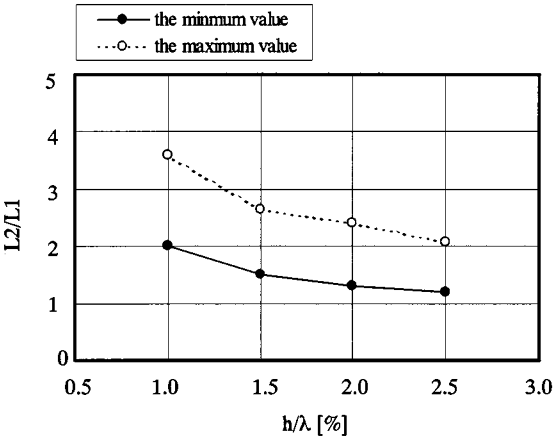

Fig. 14. Region of the finger-width ratio, where the DWSF–SPUDT improves the insertion loss, as a function of h/λ.

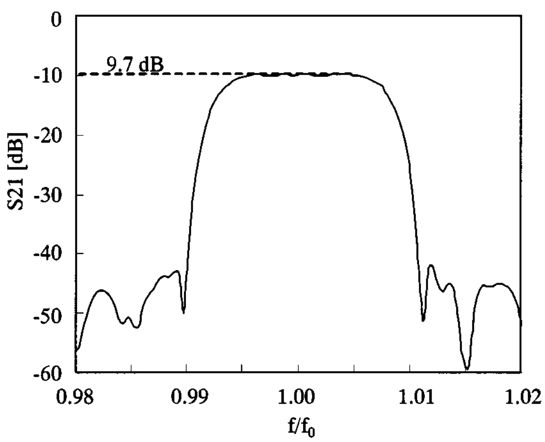

(a)

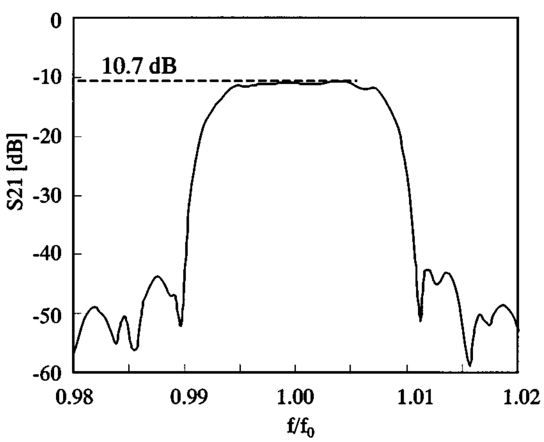

(b)

Fig. 15. Frequency response (S_{21}) of the filter using: (a) the DWSF–SPUDT and (b) EWC–SPUDT.

Fig. 14 shows the region of the finger-width ratio dependence on the metallization thickness in which the DWSF–SPUDT improves the insertion loss. The dashed line indicates the maximum finger-width ratio and the solid line indicates the minimum finger-width ratio. Between the two lines, the insertion loss is smaller than that of EWC–SPUDT. The region in Fig. 14 is different from those with the finger-width ratios used in Figs. 12 and 13. This means that the tradeoff relation between the electrical $1/Q$ factor and directivity is dependent on the metallization thickness. The insertion loss of the DWSF–SPUDT is minimized if a finger-width ratio between the solid and dashed lines is applied to the filters. The minimum critical geometry is about 0.5 μm, thus, a DWSF–SPUDT using $L2/L1 = 3.0$ can be applied up to 400 MHz. At larger metallization thickness, $L2/L1$ would need to be smaller, as shown in Fig. 14. In the case of $L2/L1 = 2.0$, the DWSF–SPUDT could be used for practical applications up to 500 MHz.

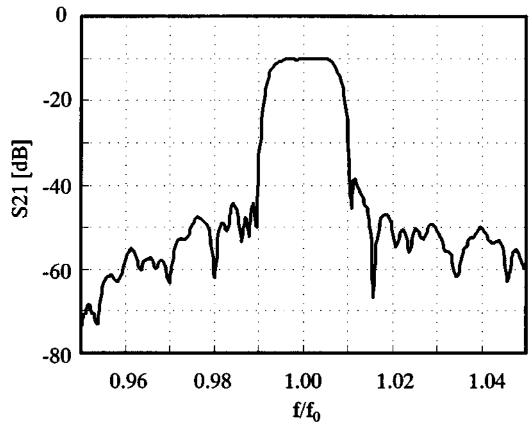

(a)

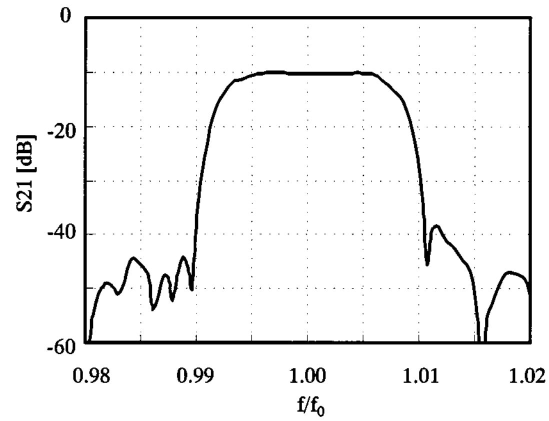

(b)

Fig. 16. Experimental results for the filter using the DWSF–SPUDT design. (a) Performance over a wide frequency span. (b) Expanded span around f_0.

IV. Simulated and Measured Perfomances of the Filter

In this section, the performance of the DWSF–SPUDT has been confirmed through simulation and by experimentation. Fig. 15 shows the simulation results of the SAW filters for a wide-band CDMA application. Fig. 15(a) indicates the insertion loss of the filter using the DWSF–SPUDT, and Fig. 15(b) indicates the insertion loss of the filter using the EWC–SPUDT. Here, $h/\lambda = 1.5\%$ and a metallization ratio is 0.5. A DWSF–SPUDT with a finger-width ratio of $L2/L1 = 1.8$ is used. An impedance matching circuit was used, composed of a series capacitor and parallel inductor. The source and load impedances were 50 Ω. The Q-value of the inductors used for the simulations was 35. The insertion loss of the DWSF–SPUDT filter is 9.7 dB. On the other hand, the insertion loss of the EWC–SPUDT filter is 10.7 dB. The insertion loss of the filters originates due to the conversion loss of electromechanical energy, directivity loss, propagation loss, ohmic loss of the electrodes, and matching loss. The DWSF–SPUDT was designed using the tradeoff relation between the $1/Q$ factor and directivity. With the particular design parameters used, the conversion loss was improved, but the directivity loss was degraded. As the result of the present simulations, it is confirmed that the DWSF–SPUDT filter can improve the insertion loss.

The performance of an experimental DWSF–SPUDT filter constructed on an ST-cut quartz substrate is shown in Fig. 16. The parameters used and the design of the filter are the same as in the simulation used for Fig. 15. The filter size is a 6 mm $\times$ 3.5 mm package. Fig. 16(a) shows the performance over a wide frequency span, while Fig. 16(b) shows an expanded span around f_0. The insertion loss is 9.4 dB. A passband ripple is very flat, which is less than 1 dB in 3.84-MHz bandwidth, and a high rejection near passband have been realized. The passband characteristic was flat. Therefore, an excellent filter performance using the DWSF–SPUDT is obtained. These results agree well with the simulation results, as shown in Fig. 16.

V. Conclusions

A new design concept of an SPUDT has been investigated in this paper based on a DWSF structure with four electrodes per wavelength. A symmetrical radiation conductance is obtained by adjusting the electrode finger positions. For this SPUDT, the electrical $1/Q$ factor and directivity of a SAW are characterized by the ratio of the wide finger width divided by the narrow finger width. The optimum finger-width ratio has been determined from the point-of-view of both the electrical $1/Q$ factor and directivity. As a result, an optimum DWSF–SPUDT filter with excellent performance, offering 1-dB improvement in the insertion loss and a flat in-band characteristic, can be obtained. The application of the DWSF–SPUDT could prove very attractive for an IF filter in digital cellular applications.

Acknowledgment

The authors would like to thank T. Ishida, Director, Matsushita Electric Industrial (MEI) Corporation Ltd., Osaka, Japan, H. Kosugi, Device Engineering Development Center, MEI Ltd., Osaka, Japan, and Dr. K. Ogawa, Device Engineering Development Center, MEI Ltd., Osaka, Japan, for providing the opportunity to carry out these studies and for their encouragement. The authors also thank K. Tazuke, MEI Ltd., Osaka, Japan, and Y. Murase, MEI Ltd., Osaka, Japan, for their support.

References

[1] K. Hamma and B. J. Hunsinger, “A triple transit suppression technique,” in *Proc. IEEE Ultrason. Symp.*, 1976, pp. 328–331.

[2] C. S. Hartmann, P. V. Wright, R. J. Kansy, and E. M. Garber, “An analysis of SAW inter-digital transducers with internal reflections and the application to the design of single-phase unidirectional transducers,” in *Proc. IEEE Ultrason. Symp.*, 1982, pp. 40–45.

[3] P. V. Wright, “The natural single-phase unidirectional transducer: A new low-loss SAW transducer,” in *Proc. IEEE Ultrason. Symp.*, 1985, pp. 58–63.

[4] T. Kodama, H. Kawabata, Y. Yasuhara, and H. Sato, “Design of low-loss SAW filters employing distributed acoustic reflection transducers,” in *Proc. IEEE Ultrason. Symp.*, 1986, pp. 59–64.

[5] C. S. Hartmann and B. P. Abbott, “Overview of design challenges for single phase unidirectional SAW filters,” in *Proc. IEEE Ultrason. Symp.*, 1989, pp. 79–89.

[6] B. J. Hunsinger and K. Hanma, “Surface acoustic wave device with reflection suppression,” U.S. Patent 4 162 465, July 24, 1979.

[7] P. V. Wright, D. F. Thompson, and R. E. Chang, “Single-phase unidirectional transducers employing uniform-width dithered electrodes,” in *Proc. IEEE Ultrason. Symp.*, 1995, pp. 27–32.

[8] K. Hashimoto, *Surface Acoustic Wave Devices in Telecommunications*. Berlin, Germany: Springer-Verlag, 2000.

[9] D. P. Morgan, *Surface-Wave Devices for Signal Processing*. Amsterdam, The Netherlands: Levier, 1985.

[10] P. V. Wright, “A uniformly-sampled single-phase unidirectional transducer with sub-nyquist spatial sampling,” in *Proc. IEEE Ultrason. Symp.*, 1992, pp. 61–66.

[11] W. R. Smith, H. M. Gerard, J. H. Collins, and T. M. Reeder, “Analysis of interdigital surface wave transducers by use of an equivalent circuit model,” *IEEE Trans. Microwave Theory Tech.*, vol. MTT-17, pp. 856–864, Nov. 1969.

[12] H. Nakamura, T. Yamada, T. Igaki, K. Nishimura, T. Ishizaki, and K. Ogawa, “A practical SPUDT design for SAW filters with different-width split-finger interdigital transducers,” presented at the *IEEE Ultrason. Symp.*, 2000.

Hiroyuki Nakamura (M’01) was born in Wakayama, Japan, in 1969. He received the B.S. and M.S. degrees in electrical engineering from Tohoku University, Tohoku, Japan, in 1993 and 1995, respectively.

In 1995 he joined the Matsushita Electric Industrial Corporation Ltd., Osaka, Japan, where he has been involved in research and development on microwave circuitry and components, especially those based on SAW filters for cellular radio communications.

Mr. Nakamura is a member of the Institute of Electrical, Information and Communication Engineers (IEICE), Japan.

Toru Yamada (M’96) was born in Mie, Japan, in 1967. He received the B.S. and M.S. degrees in electrical engineering from Kyoto University, Kyoto, Japan, in 1989 and 1991, respectively.

In 1991 he joined the Matsushita Electric Industrial Corporation Ltd., Osaka, Japan, where he has been involved in the research and development of microwave circuitry and components, especially those based on SAW filters for cellular radio communications.

Mr. Yamada is a member of the Institute of Electrical, Information and Communication Engineers (IEICE), Japan.

Toshio Ishizaki (M’90–SM’99) was born in Kagawa, Japan, on May 24, 1958. He received the B.S., M.S., and doctorate of engineering degrees from Kyoto University, Kyoto, Japan, in 1981, 1983, and 1998, respectively.

In 1983, he joined the Matsushita Electric Industrial Corporation Ltd., Osaka, Japan, where he has been involved in research and development on microwave circuitry and components, especially on microwave dielectric filters and SAW filters for cellular radio communications.

Dr. Ishizaki is a member of the Institute of Electrical, Information and Communication Engineers (IEICE), Japan. He was the recipient of the 1998 OHM Technology Award presented by the Promotion Foundation for Electrical Science and Engineering, Japan.

Kazunori Nishimura was born in Hyogo, Japan, in 1963. He received the B.S. degree from the Himeji Institute of Technology, Himeji, Japan, in 1986, and the M.S. degree from Osaka University, Osaka, Japan, in 1988.

In 1988, he joined the Matsushita Electronic Components Corporation Ltd., Osaka, Japan, where has been involved in the development SAW devices.